Intermediates in the reduction of the antituberculosis drug PA-824, (6*S*)-2-nitro-6-{[4-(trifluoromethoxy)benzyl]oxy}-6,7-dihydro-5*H*-imidazo[2,1-*b*][1,3]oxazine, in aqueous solution†

Robert F. Anderson,*[a,b] Sujata S. Shinde,[a,b] Andrej Maroz,[a] Maruta Boyd,[b] Brian D. Palmer[b] and William A. Denny[b]

Received 1st February 2008, Accepted 11th March 2008
First published as an Advance Article on the web 9th April 2008
DOI: 10.1039/b801859f

The reduction chemistry of the new anti-tuberculosis drug PA-824, together with a more water-soluble analogue, have been investigated using pulse and steady-state radiolysis in aqueous solution. Stepwise reduction of these nitroimidazo-dihydrooxazine compounds through electron transfer from the $CO_2^{\bullet-}$ species revealed that, unlike related nitroimidazoles, 2-electron addition resulted in the reduction of the imidazole ring in preference to the nitro group. In mildly acidic solution a nitrodihydroimidazo intermediate was formed, which was reduced further to the amine product. In both alkaline and neutral solution, an intermediate produced on 2-electron reduction was resistant to further reduction and reverted to parent compound on extraction or mass spectrometric analysis of the solution. The unusual reduction chemistry of these nitroimidazole compounds, exhibiting ring over nitro group reduction, is associated with alkoxy substitution in the 2-position of a 4-nitroimidazole. The unique properties of the intermediates formed on the reduction of PA-824 need to be considered as playing a possible role in its bactericidal action.

Introduction

Multi-drug resistance has become a major setback in controlling tuberculosis, a disease which kills approximately two million people annually and is the greatest single infection worldwide.[1] There is an urgent need for new drug leads to be identified, followed by the rational design of improved therapeutics. PA-824, ((6*S*)-2-nitro-6-{[4-(trifluoromethoxy)benzyl]oxy}-6,7-dihydro-5*H*-imidazo[2,1-*b*][1,3]oxazine) (**1**) (Scheme 1), shows good bactericidal activity against both latent and replicating *Mycobacterium tuberculosis*,[2] is active in preclinical murine models[2–4] and entered Phase I clinical trial in 2005. The mechanism by which **1** imparts its bactericidal effect is poorly understood, but has been shown to be dependent on drug activation by a specific protein, Rv3547,[5] which in turn is sensitive to F_{420}-dependent glucose-6-phosphate dehydrogenase (FGD) activity in the bacterium. Analogy between the activity of the 5-nitroimidazole, metronidazole (**6**), and **1** is often drawn, simply on the basis of both compounds being nitroimidazoles.[6] The reduction chemistry of the majority of nitroaromatics, including **6** and the 4-nitroimidazole **5**, is known to be dominated by the stepwise reduction of the nitro group, with intermediates such as the nitroso form being cytotoxic nucleophiles. Evidence for multi-electron reduction of **1** has come from voltammetric studies, which reveal reduction of both the nitro group[7] and the imidazole ring.[8] In these studies, aprotic solvents are used to stabilize the reduced intermediates for investigation. While **6** has been extensively studied in protic solvents using electrochemical[9,10] and radiolytic techniques,[11,12] there has been little work on identifying the reduction intermediates and products formed from **1**. Recently, a stable metabolite of the related clinical candidate drug OPC-67683, a nitroimidazo-dihydrooxazole, has been identified as the desnitro analogue;[13] however, there is no information on more active intermediates which could possibly play a role in the cytotoxicity of this drug. It is known that in aqueous solution 5-nitroimidazoles, such as **6**, are generally of higher one-electron reduction potential, $E(1)$, than 4-nitroimidazoles;[14] however, the influence of the fused oxazine ring on $E(1)$ of **1** is unknown. In this study we have used both pulse and steady-state radiolysis in aqueous solution to investigate the reduction of **1**, its more soluble analogue without the lipophilic sidechain (**2**) and the related compound 2-methoxy-1-methyl-4-nitro-1*H*-imidazole (**4**). Also, UV-vis spectral studies and mass spectrometry analysis are used to follow both the reduction of the compounds and identify the intermediates/products which

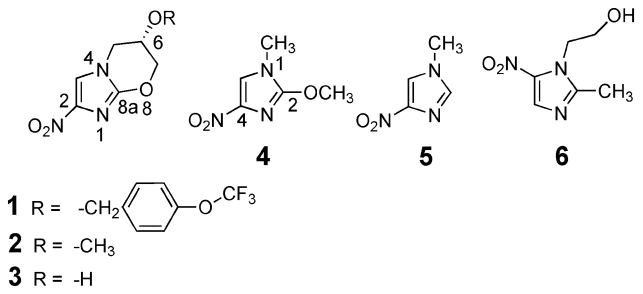

Scheme 1

[a]*Department of Chemistry, The University of Auckland, Private Bag 92019, Auckland, 1142, New Zealand. E-mail: r.anderson@auckland.ac.nz; Fax: +64 9 3737422; Tel: +64 9 3737599 extn 88315*
[b]*Auckland Cancer Society Research Centre, The University of Auckland, Private Bag 92019, Auckland, 1142, New Zealand*

† Electronic supplementary information (ESI) available: Isotropic Fermi contact couplings for radical anion of **2**. See DOI: 10.1039/b801859f

are formed. DFT calculations are carried out to gain insight on the nature of the radical species formed upon their one-electron reduction.

Results and discussion

(a) Radical absorption spectra

One-electron reduction of **1** and **2** was carried out by electron transfer from the $CO_2^{\bullet-}$ species, which reacted with both compounds with a rate constant of 2.0×10^9 M^{-1} s^{-1}. The obtained time-resolved difference spectra (between the pre-irradiated parent compound and its radical) are the same for both compounds over a wide range in pH (4–11), and a representative spectrum is presented in Fig. 1. The radical species measured 20 μs and 10 ms after the pulse, **I**, shows a narrow increase in absorption centred at 270 nm, a broad but weaker absorption at 440 nm and bleaching centred at 340 nm. Spectral changes are seen with increasing acidity below pH 4 as an increase in absorption at 290 nm and a decrease at 415 nm, leading to a proposed radical pK_a of **I** of 1.65 ± 0.2 (Fig. 1, Insert B).

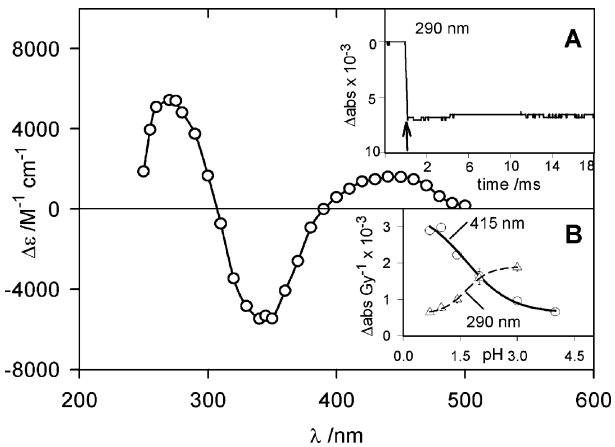

Fig. 1 Transient absorption spectra (presented as the change in absorbance relative to unirradiated solution) observed following the pulse radiolysis (2.5 Gy in 200 ns) of N_2O-saturated aqueous solution containing **2** (100 μM), sodium formate (0.1 M) buffered at pH 7 (phosphate, 5 mM). Identical measurements were made at 50 μs and 10 ms (○) following the electron pulse. Insert A: Oscilloscope trace of the change in transmittance *vs.* time following pulse radiolysis (arrow). Insert B: Changes in absorption with pH.

One-electron reduction of **1** and **2** was also carried out using the e^-_{aq} in deaerated solutions containing 2-methylpropan-2-ol (0.1 M) as an $^{\bullet}OH/H^{\bullet}$ radical scavenger. This produces what is generally considered to be a relatively inert alkyl radical (Fig. 2). The same spectrum as for **I** above is initially produced followed over 5 ms by a shift in the absorption centred at 270 nm to a greater absorption at 290 nm. The change in radical absorption was investigated by studying the reaction of the alkyl radical of 2-methylpropan-2-ol (produced in N_2O-saturated solution) with **2**. The alkyl radical was found to react slowly (*ca.* 7 ± 1.5 × 10^6 M^{-1} s^{-1}) to produce **II**, which has an absorption band in the 270–290 nm region with an extinction coefficient of *ca.* 1500 M^{-1} cm^{-1} (Fig. 3). The absorption of **II** can account for most of the spectral changes observed in Fig. 2 and possesses a pK of

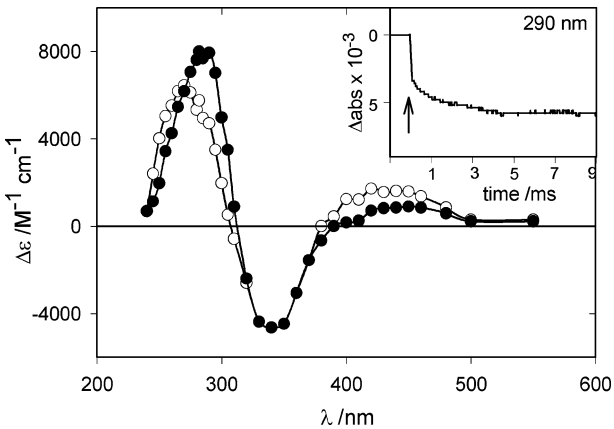

Fig. 2 Transient absorption spectra observed following the pulse radiolysis (2.5 Gy in 200 ns) of deaerated aqueous solution containing **1** (100 μM), 2-methylpropan-2-ol (0.1 M) buffered at pH 10 (pyrophosphate, 5 mM). Measurements made at 2 μs (○) and 5 ms (●) following the electron pulse. Insert: Oscilloscope trace of the change in transmittance *vs.* time following pulse radiolysis (arrow).

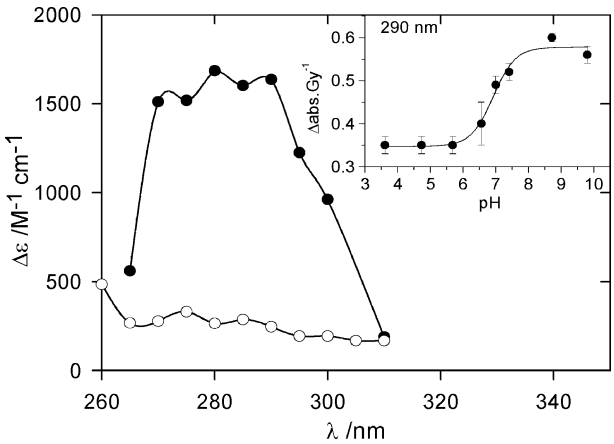

Fig. 3 Transient absorption spectra observed following the pulse radiolysis (2.5 Gy in 200 ns) of N_2O-saturated aqueous solution buffered at pH 10 (pyrophosphate, 5 mM) containing (a) 2-methylpropan-2-ol (0.1 M), measured at 1 μs (○), and (b) **1** (100 μM) and 2-methylpropan-2-ol (0.1 M), at 5 ms (●). Insert: Change in absorbance *vs.* pH for (b).

6.9 ± 0.1 (insert Fig. 3). However, some radical–radical reactions between **I** and the alkyl radical occur under pulse radiolysis conditions, as evidenced by the decrease in the visible absorption band at 440 nm after 5 ms.

(b) Conductivity measurements

Changes in conductance following pulse radiolysis were compared to those observed following the oxidation of DMSO in N_2O-saturated solution as a standard. When the differences in radical yield are taken into account, similar changes to that of the standard were found for the compounds in solutions adjusted to pH 4.3–5.5 with $HClO_4$ and pH 10.5 with NaOH (data not shown). Oxidation of DMSO by the $^{\bullet}OH$ radical results in the rapid formation of sulfinic acid (pK_a 2.28) which increases the conductance of the pre-pulse solution under acidic conditions, and decreases the conductance under basic conditions (due to neutralization).[15]

These results imply that the one-electron reduced species, **I**, of both **1** and **2** at pH ≥4 are radical anions.

(c) One-electron reduction potential, *E*(1)

It is widely recognized that *E*(1) at pH 7 is a controlling parameter in the activation of several classes of bioreductive drugs. Redox equilibria were established between species **I** of both **1** and **2** and the redox indicator tetraquat ($E(1) = -635 \pm 6$ mV[16]) on the 20 μs timescale following their reduction by the e^-_{aq}. Equilibrium constants, $K = 81.4 \pm 14.4$ and 102 ± 10 gave similar values for *E*(1) of -534 ± 7 mV and -527 ± 6 mV for **1** and **2** respectively. While these potentials are relatively low, restricting the range of proteins which could possibly carry out one-electron reduction of **1**, they are considerably higher than the *E*(1) of the F_{420} 5-deazaflavin cofactor at −650 mV.[17] However, 5-deazariboflavin is only known as a 2-electron competent cofactor in protein function, with a two electron reduction potential of −310 mV.[18] This fact points to the possible importance of a reduction intermediate at the 2-electron level.

If enzymatic reduction of **1** does occur in the bacterium, its radical anion would be subject to back-oxidation by O_2. We have determined this rate constant to be $1.9 \pm 0.2 \times 10^7$ M^{-1} s^{-1} from measurements of the pseudo-first-order decay rates of the radical anion absorption at 450 nm for a range of oxygen concentrations. The rate constant is similar to that measured for other 4-nitroimidazoles of similar *E*(1).[19]

(d) DFT calculations for the radical anion of 2

The distribution of the HOMO on one-electron-reduced **2** was calculated using DFT at the UB3LYP/6-31G(d,p) level. Electron distribution is shared mainly between the nitro substituent and over the C2–C3 region of the imidazole ring (using systematic numbering for **2** – see Scheme 1) (Fig. 4). The HOMO population at C3 is slightly higher than that on the N and O atoms of the nitro group, making C3 a favourable position for protonation or other electrophilic attack. The spin density distribution in the radical anion indicates that radical–radical reactions can occur at several sites on the compound; at C2 and C3 as well as at the atoms of the nitro group (see ESI†).

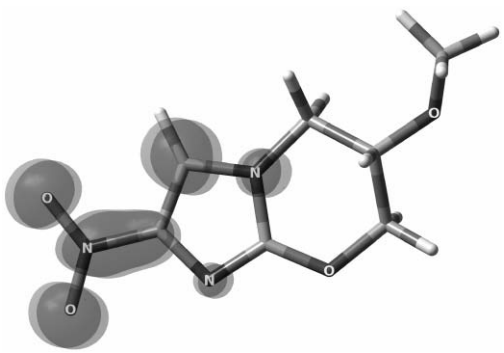

Fig. 4 HOMO of the radical anion (one-electron-reduced species) of the structure **2**, surface isovalue = 0.05. Calculated using DFT UB3LYP/6-31G(d,p)

(e) Steady-state radiolysis, HPLC and mass analysis of products

The reduction of compounds **1**, **2** and **4** by the $CO_2^{\bullet-}$ species upon accumulated radiation dose was monitored using UV-vis spectrophotometry. For **1** and **2** the loss in absorption of the parent compound, centred at 340 nm, resulted in the formation of products which absorbed maximally at lower wavelengths, with the maintenance of isobestic points. The pH-dependent spectral data for **2** is given in Fig. 5. Products could be separated from their parent compounds using HPLC but some of these, formed by radiolysis under high pH conditions, were unstable in the pH 3.5, ammonium formate–acetonitrile–water solvent used in the analysis. Typical chromatograms, obtained on the radiolysis of **1** at different pH, are displayed in Fig. 6. Converting the absorption at 340 nm into concentration and plotting its loss against radiation

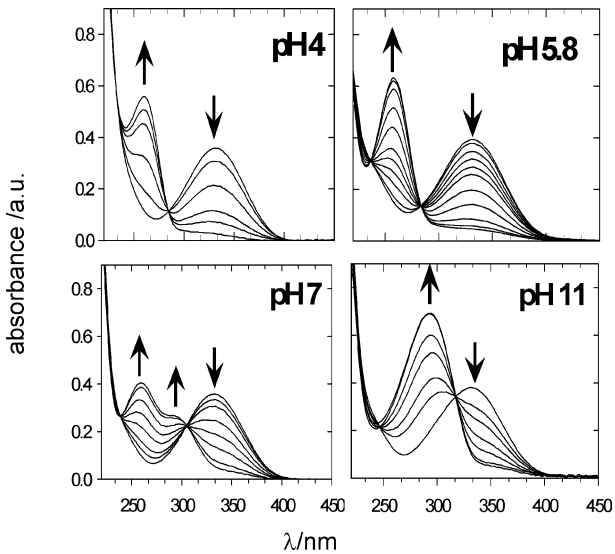

Fig. 5 Changes in UV-vis absorption spectra, observed during the γ-irradiation (absorbed doses 0–150 Gy) of N_2O-saturated aqueous solutions of the compound **2** (50 μM), containing sodium formate (50 mM) and phosphate buffer (5 mM) at different pH.

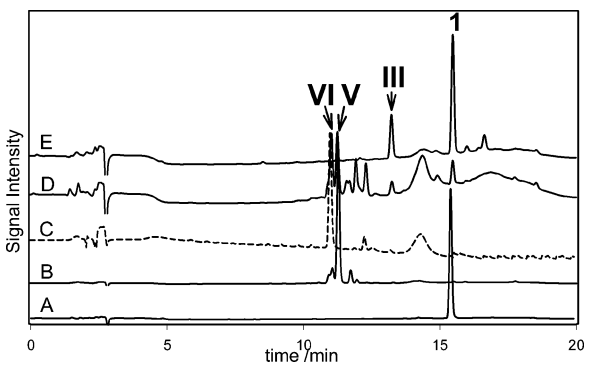

Fig. 6 Reverse-phase HPLC chromatograms (A–E) of products obtained following the reduction of **1** (~30 μM) by the $CO_2^{\bullet-}$ radical, generated in N_2O-saturated solutions containing sodium formate (50 mM) and phosphate buffer (5 mM) under different pH conditions: (A) unirradiated, (B) pH 4.0, at the 2-electron reduction level, (C) pH 4.0, 6-electron reduction, (D) pH 7.0, 2-electron reduction, and (E) pH 10.5, 2-electron reduction. The chromatograms were obtained at the λ_{max} of the products, and each chromatogram has been scaled for maximum signal intensity.

Table 1 Radiolytic yield for the loss of compounds **1**, **2**, **4** and formation of products following reduction by the $CO_2^{\bullet -}$ radical in aqueous solution

Compd (Ion mass$^+$)	pH	G_{loss}[a]/μM Gy^{-1}	λ_{max}/nm of products	Ion mass[c]/ g mol^{-1}	G_{loss}[g]/μM Gy^{-1}	λ_{max}/nm of products	Ion mass[c,h]/ g mol^{-1}
1 (360.6)	4.0	0.30 ± 0.01	*262* **V**	362.6[d]	0.13 ± 0.01	*250* **VI**	330.5[d]
1	7.0	0.23 ± 0.01	**IV**[b]	346.6			
			293 **III**	(360.6)[e,f]			
1	10.5	0.31 ± 0.01	*293* **III**	(360.6)	0[i]	—	(360.6)[f]
2 (200.4)	4.0	0.33 ± 0.01	*262* **V**	202.4[d]	0.14 ± 0.01	*250* **VI**	170.4[d]
2	5.8	0.19 ± 0.01	*262* **V**	202.4			
			IV[b]	186.4[e]			
2	7.0	0.29 ± 0.01	**IV**[b]	186.4			
			293 **III**	(200.4)[e,f]			
2	8.0	0.29 ± 0.01	*293* **III**	(200.4)[f]			
2	10.5	0.33 ± 0.01	*293* **III**	(200.4)[f]	0[i]	—	(200.4)[f]
4 (158.4)	4.0	0.34 ± 0.01	*262*	160.4[d]	0.16 ± 0.01	*258*	214.4
4	7	0.33 ± 0.01	*262*	(158.4)[f]			
			290				
4	10.5	0.62 ± 0.02	*290*	(158.4)[f]	0[i]		(158.4)[f]

[a] Loss of compounds measured at 332 nm. [b] Hydroxylamine is assumed to absorb only weakly. [c] Positive ion. [d] Only mass peak. [e] Predominant peak in mass spectrum. [f] Product reverts to parent compound upon mass spectrometry. [g] Loss of initially formed product **V** measured at 262 nm (pH 4). [h] Product arising from secondary reduction. [i] No loss in absorption at 290 nm on further irradiation.

dose enabled *G* values (radiation yield in μM Gy^{-1}) for the loss of **1** and **2** to be calculated (Table 1). Comparing these values with the *G* value of the radiolytically-produced $CO_2^{\bullet -}$ species (0.66 μM Gy^{-1})[20] indicates that that 2 electrons are required to convert all of the parent compound into products for solutions at pH ≥7. The predominant product at these pH values, **III**, identified by its strong absorption band at 293 nm, is assumed to be unstable to mass spectrometry analysis, as the same molecular mass as the parent compound was obtained on analysis. Similar spectral changes (but with a maximum absorption of the product at 295 nm at greater intensity) have been reported upon treatment of **1** with strong alkali (pH ≥12),[7] which points to it, and possibly **III**, being a product which can also be formed by hydrolysis. We have found that this product, formed by the action of alkali on **1**, only partially reforms the 332 nm band of **1** upon decreasing the pH of the solution to ≤7. Also **III** was found to be unstable over time at pH 7 (half-life *ca.* 1 h). No reduction of **III** was observed to occur upon further irradiation, *i.e.* radiolytic reduction by the $CO_2^{\bullet -}$ species was arrested at the 2-electron-reduced level. This is markedly different to observations made with other nitroimidazoles where reduction by the $CO_2^{\bullet -}$ species in steady-state radiolysis is to the 4-electron-reduced level.[12] Under acidic conditions, pH 4, a single product is formed with slightly greater than 2-electron stoichiometry and absorbs maximally at 262 nm. Mass analysis of this product, **V**, shows it to have gained 2 mass units over both **1** and **2**. Further reduction of **V** with 4 electrons leads again to the formation of **VI**, which absorbs maximally at 250 nm. This process most likely proceeds *via* intermediates **IIb**, **V**, and reduction of the nitro group to the hydroxylamine, followed by water elimination to form the amine, **VI**. The molecular mass and overall 6-electron stoichiometry identifies this final product as the amine derivative of the compounds. Reduction of **1** and **2** at pH 5.8 leads to the formation of a different predominant product, **IV**, with *ca.* 4-electron stoichiometry. Mass analysis of **IV** is consistent with the formation of the hydroxylamine derivative of the compounds. (A minor amount of **IV**, relative to **III** is also formed at pH 7). The hydroxylamine is expected to have a UV-vis absorption spectrum of much lower intensity than that of the parent nitroimidazole[12] but this could not be determined from our experiments. Thus a range of different intermediates and products are formed *via* multiple 1-electron reduction events of **1** and **2**, which are dependent on the pH of the solution (Scheme 2). Similar data was obtained for **4** in regard to product formation at the 2-electron reduction level. However, products produced on further reduction of **4** must fragment and undergo radical–radical events. since the major product is of increased mass. A product with the same increased mass was obtained upon the 6-electron reduction of **5**, which underlines the instability of these reduced small-sized nitroimidazoles in the mass spectrometer.

The above results point to the importance of the oxazine ether ring in the reduction chemistry of **1** and **2**. Voltammetric studies in protic media on the reduction of the 2-methylhydroxy analogue of **5**[21] showed it to exhibit typical nitroimidazole behaviour, *i.e.* proceeding through the formation of its radical anion, followed by further reduction and disproportionation reactions to form the nitroso, hydroxylamine and amine derivatives. We also find that the reduction of **5** under our experimental conditions did not lead to the formation of either **III** or **V** (data not shown).

(f) NMR studies on products formed by steady-state radiolysis

NMR analysis was attempted on the single product **V** produced upon the reduction of **2** (1.5 mM) by the $CO_2^{\bullet -}$ species under low pH conditions. The product formed proved to be much more polar than **2** and resisted extraction from the aqueous solution into non-protic solvents. The solution was concentrated to dryness and the residue purified by reverse phase semi-preparative HPLC, using a buffer-free eluant. A single peak almost eluting with the void volume of the column was collected, concentrated to dryness, and the residue was subjected to detailed ^{1}H and ^{13}C NMR analysis (1D and 2D). Despite eluting as a single peak on HPLC, the NMR analysis indicated the presence of two major products.

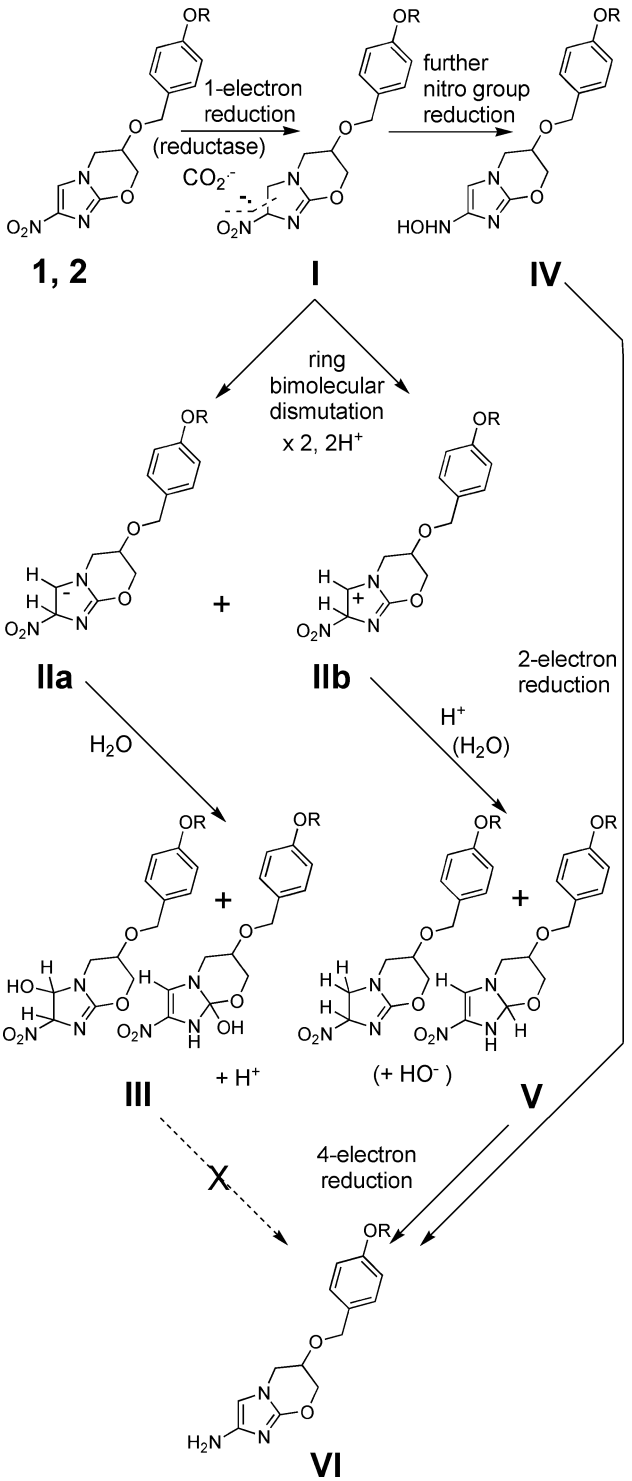

Scheme 2

Resonances associated with the 6-membered oxazine ring were generally maintained in both compounds, indicating this ring to be intact. One component of the mixture contained a singlet at δ 8.25 ppm in the ^{1}H spectrum, which correlated to a signal at δ 165.0 ppm in the ^{13}C spectrum. This is proposed to result from the C3 olefinic proton of the product resulting from reduction of the N1–C8a double bond. A singlet at δ 5.5 in the ^{1}H NMR spectrum (correlated to a signal at δ 80.0 ppm in the ^{13}C spectrum) is proposed to result from the new proton now at the C8a position. The resonance at δ 5.5 displayed a 3-bond coupling correlation with the carbon resonance at δ 165.0, indicating them to be in the same molecule. In the second component of the mixture an ABX coupling system in the ^{1}H NMR spectrum was consistent with the –NCH_2CHNO_2–system which would result from reduction of the C2–C3 bond. Overall, the NMR spectra are consistent with **V** containing the products resulting from reduction of each of the double bonds of the imidazole ring. This is also consistent with the observed mass of this product, being two units higher than the starting material **2**. Another possibility for this product, that it results from cleavage of the C8a–O bond of the oxazine ring, could be discounted, since an authentic sample of the alcohol which would be produced was available for comparison.

The reaction with **2** of the alkyl radical formed upon reaction of the $^{\bullet}$OH radical with 2-methylpropan-2-ol was further studied by isolating the product formed for NMR analysis. The steady-state radiolysis of a N_2O-saturated solution containing **2** (400 μM), 2-methylpropan-2-ol (0.2 M), buffered at pH 7 (5 mM phosphate) was followed spectroscopically to the point when all of **2** was lost from solution, as evidenced by the loss of the 332 nm absorption band. A scale-up preparation of 1.5 mM **2** in 1 M 2-methylpropan-2-ol was irradiated for product analysis (see Experimental). Thin layer chromatography revealed only one major product of marginally greater polarity than the starting material, and this product was recovered from the irradiation solution and purified by chromatography on silica gel. Low resolution mass spectrometry indicated the mass of the product to be 271, corresponding to the addition of 2-methylpropan-2-ol to **2**, and this was confirmed by high resolution mass spectrometry, which gave an accurate mass consistent with a formula of $C_{11}H_{17}N_3O_5$ for this material. The ^{1}NMR spectrum of the purified product showed loss of the H-3 proton of the imidazole ring, although the characteristic resonances of the 6-membered oxazine ring and methyl ether group were still present. A new exchangeable singlet suggested the presence of an isolated hydroxyl group, and a new 2-proton AB quartet centred at δ 3.1 (J = 14.1 Hz) indicated the presence of an isolated methylene group, in an environment which was moderately electron-deficient. Finally, two new three-proton singlets at ~δ 1.1 indicated the presence of two new methyl groups. Taken together, these features clearly identified the product as the 2-nitroimidazole, **VII** (Scheme 3), formed by incorporation of 2-methyl-2-propanol at the 3-position of the imidazole ring.

Conclusions

The reduction chemistry of PA-824 exhibits atypical behaviour to that of structurally related nitroimidazole compounds. Voltammetric studies[8] have shown that the imidazole ring of **1** is subject to reduction as well as the nitro group, and the present study gives new information on the sequential reduction of these moieties. Our results, obtained upon the step-wise reduction of **1**, clearly show that imidazole ring reduction occurs in preference to nitro group reduction to the 2-electron-reduced level, over a range of pH values. This behaviour can be related to the 2-alkoxy substitution of the 4-nitroimidazole ring, as parallel results on reduction are obtained with the 2-methoxy analogue, **4**. While the lipophilic side chain of **1** is most likely necessary to direct and bind the compound to a specific protein, the subsequent activation of

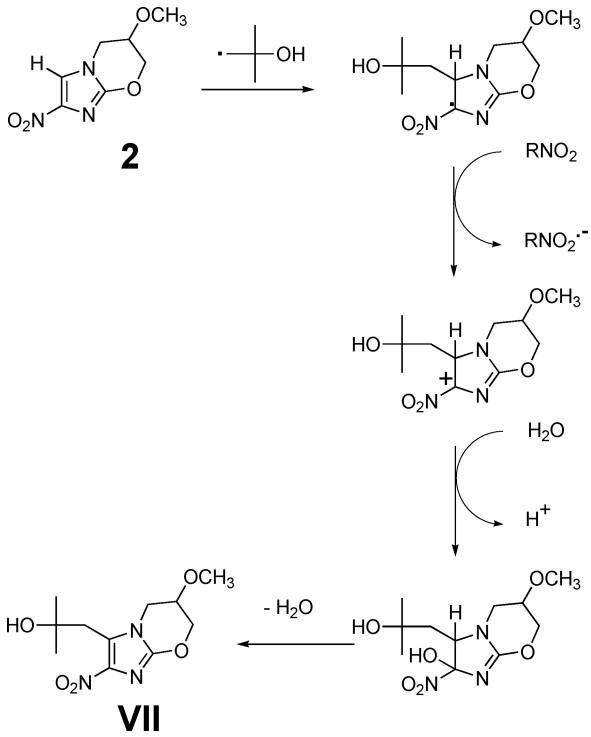

Scheme 3

the 4-nitroimidazole moiety could be a pathway leading to the bactericidal effects of **1** on *M. tuberculosis*.

It is presently unknown if the reduction intermediates characterised in this study play a role in the bactericidal action of **1**. Of particular interest are the intermediates formed at the 2-electron-reduction level, since these are produced for 4-nitroimidazoles substituted with a 2-alkoxy group. The ability of the presumed hydroxylated intermediate, **III**, to undergo facile reversion to its parent compound, **1**, raises the possibility that it might act as a hydrating agent for an unsaturated species. By analogy with fatty acid biosynthesis in *E. coli*,[22] it is thought that the biosynthesis of cell wall mycolic acids in *M. tuberculosis* proceeds through the dehydration of hydroxymycolate by a dehydratase to produce ketomycolate.[23] It has been found that treatment with **1** interferes with this process, resulting in the accumulation of the hydroxymycolate.[2] While this could arise from the inhibition of the uncharacterised dehydratase or from depletion of a cofactor, rehydration of the ketomycolate by a hydrated intermediate of **1**, such as **III**, can be considered as an alternate possibility.

Experimental

Synthesis

All reagents used were of analytical grade. Sodium formate, sodium hydroxide, perchloric acid and phosphate buffers were obtained from Merck and potassium thiocyanate from Riedel-de Haen. All other reagents were obtained from Aldrich Chemical Company. All solutions were prepared in water purified by the Millipore "Milli-Q" system. Solution pH values were adjusted using the phosphate salts (5 mM) and either NaOH or $HClO_4$ when necessary. Analyses were carried out in the Microchemical Laboratory, University of Otago, Dunedin, NZ. Melting points were determined on an Electrothermal 2300 Melting Point apparatus. ^{1}NMR spectra were obtained on a Bruker Avance 400 spectrometer at 400 MHz. Spectra are referenced to Me_4Si. Chemical shifts and coupling constants were recorded in units of ppm and Hz, respectively. High resolution mass spectra were determined on a VG-70SE mass spectrometer using an ionizing potential of 70 eV at a nominal resolution of 1000. Atmospheric pressure chemical ionisation mass spectra (APCI-MS) were determined for methanol elutions on a ThermoFinnigan Surveyor MSQ spectrometer. Solutions in organic solvents were dried with anhydrous Na_2SO_4. Solvents were evaporated under reduced pressure on a rotary evaporator. Thin-layer chromatography was carried out on aluminium-backed silica gel plates (Merck 60 F_{254}), with visualization of components by UV light (254 nm) and exposure to I_2. Column chromatography was carried out on silica gel (Merck 230–400 mesh). PA-824 (**1**)[24] and 1-methyl-4-nitro-1*H*-imidazole (**5**)[25] were synthesised as described.

(6*S*)-6-Methoxy-2-nitro-6,7-dihydro-5*H*-imidazo[2,1-*b*][1,3]-oxazine (2). Sodium hydride (0.10 g of a 60% dispersion in mineral oil, 2.57 mmol) was added in one portion to a solution of the alcohol (**3**)[24] (0.24 g, 1.29 mmol) and iodomethane (0.20 ml, 2.83 mmol) in dry DMF (5.0 ml), which had been cooled to 5 °C. After 2 min the cooling bath was removed and the solution was stirred at room temperature for 1 h. Water was added and the solution was extracted with ethyl acetate. The extract was washed five times with brine, and then worked up to give an oil which was chromatographed on silica. Elution with ethyl acetate gave **2** (0.19 g, 74%) as an off-white solid, following trituration with diethyl ether, mp 127–129 °C. ^{1}H NMR (400 MHz, DMSO-D_6) δ ppm 8.01 (s, 1H), 4.60 (dt, J = 12.0, 2.3 Hz, 1H), 4.42 (dt, J = 12.0, 0.4 Hz, 1H), 4.24–4.15 (m, 2H), 4.03–4.00 (m, 1H), 3.34 (s, 3H). APCI-MS Found: $[M + H]^+ = 200$. Found: C, 42.46; H, 4.76; N, 21.16. $C_7H_9N_3O_4$ requires C, 42.21; H, 4.55; N, 21.10%.

2-Methoxy-1-methyl-4-nitro-1*H*-imidazole (4). Methanol (1.0 ml, 0.026 mol) was added in portions under nitrogen to a stirred suspension of sodium hydride (0.27 g of a 60% dispersion in mineral oil, 6.97 mmol) in dry tetrahydrofuran (5.0 ml). After 5 min a solution of 2,4-dinitro-1-methylimidazole[26] (0.30 g, 1.74 mmol) in dry tetrahydrofuran (3.0 ml) was added and the mixture was stirred at room temperature for 2 h. Water was added and the solvents were removed *in vacuo* to leave a small volume of aqueous residue. This was extracted with ethyl acetate and the extract was worked up and chromatographed on silica. Ethyl acetate–petroleum ether 1 : 9) eluted fore-fractions, while ethyl acetate gave the product **4** (0.25 g, 91%), which crystallised from ethyl acetate–petroleum ether as white plates, mp 130–131 °C. ^{1}H NMR (400 MHz, $CDCl_3$) δ ppm 7.45 (s, 1H), 4.12 (s, 3H), 3.52 (s, 3H). APCI-MS Found: $[M + H]^+ = 158$. Found: C, 38.43; H, 4.50; N, 26.63. $C_5H_7N_3O_3$ requires C, 38.22; H, 4.49; N, 26.74%.

1-[(6*S*)-6-Methoxy-2-nitro-6,7-dihydro-5*H*-imidazo[2,1-*b*][1,3]-oxazin-3-yl]-2-methyl-2-propanol (VII). A solution of the 4-nitroimidazole (**2**) (6.0 mg, 0.030 mmol) in 1 M *tert*-butanol–water (20 ml) was γ-irradiated to 5.38 kGy. The solvents were removed *in vacuo* and the residue was partitioned between ethyl acetate and water. The extract was worked up to give an oil which was chromatographed on silica. Ethyl acetate eluted fore-fractions, while methanol–ethyl acetate (5 : 95) eluted **VII**) as a yellow oil

(3.4 mg, 47%). ^{1}H NMR (400 MHz, DMSO-D_6) δ ppm 4.69 (s, 1H, exch. with D_2O), 4.55 (ddd, J = 11.8, 2.6, 2.6 Hz,1H), 4.41 (ddd, J = 13.7, 2.2, 2.2 Hz, 1H), 4.36 (dd, J = 11.8, 0.8 Hz, 1H), 4.07 (dd, J = 13.7, 3.3 Hz, 1H), 4.00 (m, 1H), 3.34 (s, 3H), 3.16 (d, J = 14.1 Hz, 1H), 3.04 (d, J = 14.1 Hz, 1H), 1.19 (s, 3H), 1.16 (s, 3H). APCI-MS Found: $[M + H]^+ = 272$. HREI-MS Found $M^+ = 271.1165$. $C_{11}H_{17}N_3O_5$ requires 271.1168.

Methods

Pulse radiolysis experiments, at room temperature (22 ± 1 °C), were carried out using the University of Auckland's 4 MeV linear accelerator of pulse length 200 ns to deliver a typical absorbed dose of 2.5 Gy for spectral studies and 2.5–10 Gy for kinetic studies. The optical and conductivity detection systems and method of dosimetry have been described previously.[27,28] Steady-state radiolysis experiments were performed using a ^{60}Co γ-source delivering a dose rate of 7.6 Gy min^{-1}. Aqueous samples were evacuated and purged with appropriate O_2-free gasses in glass tubes for three cycles. The tubes were fitted with a side arm incorporating a supracil spectrophotometer cell for UV-vis measurements. The G(loss) values obtained by the spectrophotometric method, in which isobestic spectral points were maintained. Optical spectra were recorded on an Ocean Optics HR4000GC-UV-NIR spectrometer. Product analysis was by HPLC (Agilent 1100 liquid chromatograph coupled to an Agilent 1100 diode array detector) utilizing a reverse-phase Alltima C18 column (5 μ, 150 mm × 3.2 mm i.d.) and a gradient of aqueous (0.045 M ammonium formate, pH 3.5) and organic (80% acetonitrile–MilliQ water) solvent phases at a flow rate of 0.5 mL min^{-1}. DFT calculations were carried out using the Gaussian 03 software package.[29]

Radiation chemistry. The radiolysis of water produces three well-characterized reactive radical species[30] used to initiate radical reactions, as well as molecular products (μM per absorbed dose of 1 Gy (J Kg^{-1}) given in parenthesis).

$$H_2O \rightarrow e_{aq}^- (0.28) + {}^{\bullet}OH (0.28) + H^{\bullet} (0.055) + H_2 (0.04) + H_2O_2 (0.07) + H^+ (0.28)$$

One-electron reductions of the compounds (A) were carried out by:

(i) the e_{aq}^-, while at the same time scavenging the oxidizing radicals with 2-methylpropan-2-ol,

$$e_{aq}^- + A \rightarrow A^{\bullet -}$$

$$^{\bullet}OH/H^{\bullet} + (CH_3)_3COH \rightarrow H_2O/H_2 + {}^{\bullet}CH_2(CH_3)_2COH$$

(ii) electron transfer from the $CO_2^{\bullet -}$ species (E^0 $CO_2/CO_2^{\bullet -}$) = −1.90 V[31]) in N_2O-saturated solutions (to quantitatively convert the e^-_{aq} to $^{\bullet}OH$ radicals) containing 50 mM sodium formate, to convert the $^{\bullet}OH$ radicals and H-atoms to $CO_2^{\bullet -}$.

$$N_2O + e_{aq}^- \rightarrow {}^{\bullet}OH + OH^- + N_2$$

$$^{\bullet}OH (H^{\bullet}) + HCOO^- \rightarrow H_2O (H_2) + CO_2^{\bullet -}$$

$$CO_2^{\bullet -} + A \rightarrow A^{\bullet -} + CO_2 + H^+$$

Radical spectra are presented as the change in extinction coefficient *vs.* wavelength, relative to the unreduced compound, by converting the changes in absorption due to the radical yields of the e_{aq}^- (0.28 μM Gy^{-1})[30] and $CO_2^{\bullet -}$ (0.66 μM Gy^{-1}).[20]

One-electron reduction potentials, E(1). The one-electron reduction potentials of **1** and **2**, E(A/A$^{\bullet -}$), *vs.* NHE, were determined at pH 7.0 (5 mM phosphate buffer) by establishing redox equilibria between three mixtures of the one-electron-reduced compounds and the reference compound tetraquat (E(TeQ^{2+}/TeQ$^{+\bullet}$) = −635 ± 7 mV)[16] and calculating ΔE values from the equilibrium constants, K_e, using the Nernst equation and allowing for ionic strength effects.

$$TeQ^{\bullet +} + A \underset{}{\overset{K_e}{\rightleftharpoons}} TeQ^{2+} + A^{\bullet -}$$

Acknowledgements

This work was supported by Grant 07/243 from the Health Research Council of New Zealand, and by the Global Alliance for TB Drug Development, New York. We thank Sisira Kumara for assistance with the HPLC assay.

References

1 *Global Tuberculosis Control: Surveillance, Planning, Financing*, World Health Organization, Geneva, Switzerland, 2005. Report WHO/HTM/TB/2005.
2 C. K. Stover, P. Warrener, D. R. VanDevanter, D. R. Sherman, T. M. Arain, M. H. Langhorne, S. W. Anderson, J. A. Towell, Y. Yuan, D. N. McMurray, B. N. Kreiswirth, C. E. Barry and W. R. Baker, *Nature*, 2000, **405**, 962–966.
3 A. J. Lenaerts, V. Gruppo, K. S. Marietta, C. M. Johnson, D. K. Driscoll, N. M. Tompkins, J. D. Rose, R. C. Reynolds and I. M. Orme, *Antimicrob. Agents Chemother.*, 2005, **49**, 2294–2301.
4 S. Tyagi, E. Nuermberger, T. Yoshimatsu, K. Williams, I. Rosenthal, N. Lounis, W. Bishai and J. Grosset, *Antimicrob. Agents Chemother.*, 2005, **49**, 2289–2293.
5 U. H. Manjunatha, H. Boshoff, C. S. Dowd, L. Zhang, T. J. Albert, J. E. Norton, L. Daniels, T. Dick, S. S. Pang and C. E. Barry, III, *Proc. Natl. Acad. Sci. U. S. A.*, 2006, **103**, 431–436.
6 C. E. Barry, H. I. M. Boshoff and C. S. Dowd, *Curr. Pharm. Des.*, 2004, **10**, 3239–3262.
7 C. Yáñez, S. Bollo, L. J. Núñez-Vergara and J. A. Squella, *Anal. Lett.*, 2001, **34**, 2335–2348.
8 S. Bollo, L. J. Núñez-Vergara and J. A. Squella, *J. Electroanal. Chem.*, 2004, **562**, 9–14.
9 R. J. Knox, R. C. Knight and D. I. Edwards, *Biochem. Pharmacol.*, 1983, **32**, 2149–2156.
10 J. A. Squella, S. Bollo and L. J. Núñez-Vergara, *Curr. Org. Chem.*, 2005, **9**, 565–581.
11 P. Wardman, *Environ. Health Perspect.*, 1985, **64**, 309–320.
12 P. Wardman, R. F. Anderson, E. D. Clarke, N. R. Jones, A. I. Minchinton, K. B. Patel, M. R. L. Stratford and M. E. Watts, *Int. J. Radiat. Oncol., Biol., Phys.*, 1982, **8**, 777–780.
13 M. Matsumoto, H. Hashizume, T. Tomishige, M. Kawasaki, H. Tsubouchi, H. Sasaki, Y. Shimokawa and M. Komatsu, *PLoS Med.*, 2006, **3**, 2131–2144.
14 P. Wardman and E. D. Clarke, *J. Chem. Soc., Faraday Trans. 1*, 1976, **72**, 1377–1390.
15 K.-D. Asmus and E. Janata, in *The study of fast processes and transient species by electron pulse radiolysis*, ed. J. H. Baxendale and F. Busi, D. Reidel Publishing Company, Dordrecht, 1982, vol. 86, pp. 91–113.
16 R. F. Anderson, *Ber. Bunsen-Ges. Phys. Chem.*, 1976, **80**, 969–972.
17 G. Blankenhorn, *Eur. J. Biochem.*, 1976, **67**, 67–80.
18 C. Walsh, *Acc. Chem. Res.*, 1986, **19**, 216–221.
19 P. Wardman and E. D. Clarke, *Biochem. Biophys. Res. Commun.*, 1976, **69**, 942–949.
20 Q. G. Mulazzani, M. Venturi, M. Z. Hoffman and M. A. J. Rodgers, *J. Phys. Chem.*, 1986, **90**, 5347–5352.

21 C. Yañez, J. Pezoa, M. Rodriguez, L. J. Núñez-Vergara and J. A. Squella, *J. Electrochem. Soc.*, 2005, **152**, J46–J51.
22 K. Magnuson, S. Jackowski, C. O. Rock and J. E. Cronan, *Microbiol. Rev.*, 1993, **57**, 522–542.
23 C. E. Barry, R. E. Lee, K. Mdluli, A. E. Sampson, B. G. Schroeder, R. A. Slayden and Y. Yuan, *Prog. Lipid Res.*, 1998, **37**, 143–179.
24 W. R. Baker, C. Shaopei and E. L. Keeler, *US Patent*, 5668127 (PathoGenesis Corp), 16 Sept 1997.
25 P. Benjes and R. Grimmett, *Heterocycles*, 1994, **37**, 735–738.
26 I. J. Stratford, G. E. Adams, C. Hardy, S. Hoe, P. O'Neill and P. W. Sheldon, *Int. J. Radiat. Biol.*, 1984, **46**, 731–745.
27 R. F. Anderson, W. A. Denny, W. Li, J. E. Packer, M. Tercel and W. R. Wilson, *J. Phys. Chem. A*, 1997, **101**, 9704–9709.
28 R. F. Anderson, S. S. Shinde, M. P. Hay, S. A. Gamage and W. A. Denny, *J. Am. Chem. Soc.*, 2003, **125**, 748–756.
29 M. J. Frisch, G. W. Trucks, H. B. Schlegel, G. E. Scuseria, M. A. Robb, J. R. Cheeseman, J. A. Montgomery, Jr., T. Vreven, K. N. Kudin, J. C. Burant, J. M. Millam, S. S. Iyengar, J. Tomasi, V. Barone, B. Mennucci, M. Cossi, G. Scalmani, N. Rega, G. A. Petersson, H. Nakatsuji, M. Hada, M. Ehara, K. Toyota, R. Fukuda, J. Hasegawa, M. Ishida, T. Nakajima, Y. Honda, O. Kitao, H. Nakai, M. Klene, X. Li, J. E. Knox, H. P. Hratchian, J. B. Cross, V. Bakken, C. Adamo, J. Jaramillo, R. Gomperts, R. E. Stratmann, O. Yazyev, A. J. Austin, R. Cammi, C. Pomelli, J. Ochterski, P. Y. Ayala, K. Morokuma, G. A. Voth, P. Salvador, J. J. Dannenberg, V. G. Zakrzewski, S. Dapprich, A. D. Daniels, M. C. Strain, O. Farkas, D. K. Malick, A. D. Rabuck, K. Raghavachari, J. B. Foresman, J. V. Ortiz, Q. Cui, A. G. Baboul, S. Clifford, J. Cioslowski, B. B. Stefanov, G. Liu, A. Liashenko, P. Piskorz, I. Komaromi, R. L. Martin, D. J. Fox, T. Keith, M. A. Al-Laham, C. Y. Peng, A. Nanayakkara, M. Challacombe, P. M. W. Gill, B. G. Johnson, W. Chen, M. W. Wong, C. Gonzalez and J. A. Pople, *GAUSSIAN 03 (Revision C.02)*, Gaussian, Inc., Wallingford, CT, 2004.
30 G. V. Buxton, C. L. Greenstock, W. P. Helman and A. B. Ross, *J. Phys. Chem. Ref. Data*, 1988, **17**, 513–886.
31 H. A. Schwarz and R. W. Dodson, *J. Phys. Chem.*, 1989, **93**, 409–414.

